ICAS-80-2.3

ADVANCED COMBAT AIRCRAFT WING DESIGN

by

B. Probert
British Aerospace - Aircraft Group
Senior Aerodynamicist
Warton Division
Warton
Preston
Lancs
PR4 1AX
U.K.

D. R. Holt
British Aerospace - Aircraft Group
Principal Aerodynamicist
Kingston-Brough Division
Brough
North Humberside
HU15 1EQ
U.K.

1. Abstract

The paper considers various means of achieving a typical set of design requirements for a combat aircraft, ranging from variable sweep options to a fixed wing configuration. It is shown that with the aid of transonic theoretical methods designs can be achieved which give good (L/D) values over a wide range of Mach number and lift coefficients. Use of variable sweep is a powerful means of achieving a wide range of requirements whilst use of variable camber devices has a strong influence on reconciling, often conflicting, geometric requirements especially when aeroelastic effects are taken into account. Further improvements at high lift can be achieved with slotted devices. High incidence penetration can be aided with the use of strakes and these can be designed to have only a small drag penalty at low lift coefficients. These points are illustrated by describing the design of a variable sweep and fixed wing configuration and results are described and discussed for both.

2. Introduction

Over the past few years a number of new features have figured in the designer's ability to design wing-body configurations to achieve improved aerodynamic performance. One of the most notable is the capability to predict transonic or mixed flows with shock waves, both in two and three dimensions, which has enabled the designer to design efficient configurations with the minimum amount of wind tunnel testing. It is now possible to predict the flow development at high Mach numbers, high C_L conditions in the attached flow regime and thus to design wing-body shapes to give favourable pressure distributions which virtually guarantee low drag levels. However this does not necessarily imply satisfactory behaviour in the separated flow regime, which is of great importance for combat aircraft - thus 'method development' still has a long way to go. For the previous generation of aircraft, the design was done using subcritical methods, relying on the designer's experience to make an allowance for the transonic development. Checkout could only be done in the wind tunnel. Design using subcritical methods is still being carried out and, provided that the flight envelope and the configuration being studied is not too far removed from earlier designs, can give adequate results. This is especially true of wings with high aspect ratios and moderate, $\Lambda < 35^{\circ}$ sweep. However, for military aircraft configurations with low aspect ratio, often highly tapered wings and a broad flight envelope, both subsonic and supersonic, transonic methods are virtually essential if good design is to be achieved economically.

Whatever methods are available the options open to the designer in his aim to achieve a target set of requirements are many and varied. Here we consider only a few of them. The dominant factor, apart from wing loading, is the choice of wing planform, especially wing sweep and aspect ratio. If the requirements are wide in scope the best solution from the aerodynamic point of view may well be a wing with variable sweep capability. A secondary factor is wing thickness with the choice of this probably dominated by supersonic and structural requirements. The value used will mainly depend on wing sweep (supersonic) and aspect ratio (structural) so that a variable sweep wing may well have a thicker section than that of an equivalent fixed wing option, with increased sweep compensating for the increased (t/c) for the supersonic case. The increased thickness of the variable sweep option would also allow the use of a higher aspect ratio, without incurring a wing weight penalty, hence benefiting induced drag.

Design considerations for attached flow and low drag at both high and low lift coefficients yield conflicting requirements for leading and trailing edge camber. Variable camber overcomes this problem. The need for such systems is likely to be greater for the fixed wing configuration, since the powerful wing sweep option is no longer available. In either case, design of wings to give good manoeuvre performance is best achieved if a smooth curvature distribution can be maintained over the wing surface. To achieve this, variable camber flexible skin schemes can be used, with appropriate deflections which keep upper or lower surfaces smooth at high or low lift coefficients respectively.

With aircraft capable of supersonic flight the resulting thin wings, and high design loadings involved, imply that the effect of aeroelasticity cannot be ignored. It is fortunate that, from the swept back wing design point of view, this effect acts in a beneficial manner reducing loading over the outer wing region where flow separations and increased drag are often a problem. To some extent this occurs naturally, dependent on planform/thickness, but as has been widely reported it may be possible to so design the wing structure that natural aeroelastic deformation will achieve the required shape which will give optimum performance.

Such detailed design work can lead to configurations giving high levels of sustained 'g' capability at low and moderate altitudes, by virtue of good (L/D) values, but not necessarily high levels of lift. High lift penetration can be gained through the use of leading edge strakes, which effectively increase the stalling angle of

the basic wing. As yet there is no proper theoretical treatment for such configurations but here they are classified into two types - 'interfering' and 'non-interfering'. Further improvements to high lift performance are obviously obtained using downward deflections of high lift devices, but with the effectiveness of various types of device varying over the flight envelope.

Having gone through a design procedure the resulting wing shape may be of a fairly complicated nature, consisting of many control stations, complicated camber/twist variations etc. This could lead to difficulties in manufacture or with some weight and/or cost penalties, thus even at an early stage in the design process thought should be given to the practicalities of wing manufacture.

This paper deals with each of the above points but first some general observations on design requirements and means of achieving them are made before proceeding to describe the design of specific configurations.

3. Design Requirements

Typical design requirements, which have an influence on wing design are shown in Figure 1. Here we have specific sustained manoeuvre requirements, which are at moderate altitude at both subsonic and supersonic speeds, 1g flight conditions (subsonic → supersonic) and at the low Mach number end the requirements for as high an attained g capability as possible. Four of the points have been marked and will be taken to illustrate the different flow features, and possible problem areas, which the designer is likely to meet.

Point 'A', a high subsonic Mach number, high 'g' point is often taken as the primary design point and it is here that the advances in numerical methods can give the greatest advantages. This is illustrated in the upper figure of Figure 2, which shows a comparison of predicted chordwise pressures between 'old' and 'new' technologies at equal C_L conditions. The 'old' is typified by a strong shock wave near mid chord, verging on the strength to give boundary layer separation, and with little rear loading. The 'new' has a smaller leading edge suction peak, a long isentropic recompression region leading to a further back, weaker, shock wave. The amount of rear loading is also greatly increased. The result is a tenfold reduction in wave drag as shown in the right hand figure.

Point 'B', representative of a high speed dash (subsonic), low C_L condition, could well have a pressure distribution of the form shown in Fig. 2(b) if the aerofoil of Point 'A' is used, unchanged. At low C_L the rear loading would have to be balanced by an opposing force over the front of the chord, which leads to high suction levels over the lower surface leading edge, and to shock waves/separation in extreme cases (shown here). This will produce a deterioration in drag rise Mach number as shown on the right-hand figure, large negative C_{mo} (Trim drag and load penalty) and adverse pitch down effects. The pressure gradient in the region aft of the lower surface shock can also be a limiting feature due to possible flow separations and increased drag, but usually only for thicker civil wing type applications.

Points 'C' and 'D' have the features shown in Figure 2(c) where high C_L, and lower Mach numbers are considered. Point 'C' is typified by shock waves near 10 - 20% chord and is sensitive to details just behind the leading edge on the upper surface. Peaky aerofoils which deliberately generate high suction levels at the leading edge to improve high Mach number performance can suffer in this lower speed range due to excessive shock strengths, leading to a sudden loss in lift below the design Mach number as illustrated in the right hand figure. Careful shaping of the first 10% chord can avoid or reduce this effect.

Point 'D', at the low speed end obviously calls for some leading edge droop to reduce suction levels and here some form of high lift device is needed, at least for thin wings of moderate sweep.

3.1 Means of achieving requirements

3.1.1 Use of variable sweep

From Aerodynamic considerations the choice of variable sweep or fixed wing options will have a strong influence on the choice of design points in the wing design process. It is often the case that the designer, even of a low aspect ratio wing, will have available or have developed a two dimensional aerofoil which has many desirable features, both aerodynamic and structural. The application of this to the 3D wing is illustrated in Figure 3, which shows the separation and drag rise (C_L, M) boundaries of a fairly advanced aerofoil. Superimposed on the figure are typical 3D requirements expressed as constant 'g' locii or M^2C_L = constant boundaries, with appropriate wing sweeps annotated. Two are the high subsonic high 'g' cases, the third is the sea level dash, low C_L case. If we assume that a 2D to 3D analogy holds up to wing sweeps of 45° then such a picture can give us a guide on design points. In this particular example the lower Mach high 'g' requirement falls within the $C_{L_{MAX}}$ boundary of the section for all sweeps from $25^\circ \rightarrow 45^\circ$ but the more difficult higher Mach number case is only likely to be achieved at a wing sweep of around 45°. Thus in this case detailed 3D design should well concentrate on optimising the high Mach number, $\Lambda = 45^\circ$ case. Converting this to the 2D equivalent implies moderate design Mach number for the 2D aerofoil of around 0.7. The figure also implies that a sweep of at least 35° will be needed for the high speed dash point.

If the variable sweep option is used a number of other advantages are implied in Figure 4. This shows the typical variations of $(\text{span})^2$ and wing thickness, normalised with respect to a datum fixed wing option. Aspect ratio (specifically $(\text{span})^2$) is important in reducing drag due to lift and hence in increasing sustained performance. It has been found in combat modelling work that the Mach number of engagement reduces as the encounter proceeds, thus the variable sweep option has advantages in the low to moderate mach number corner.

At high subsonic speeds with shock waves on the wing there is a trade off between the increased aspect ratio of the variable sweep wing and the reduced thickness of the fixed wing, with no clear advantage either way. At supersonic speeds the greater sweep capability and reduced (t/c) of the variable sweep case wins out. To maximise variable sweep capability thinner wings, whilst still maintaining high aspect ratios could be considered, but would entail heavy use of composites to keep weight and stiffness to an acceptable level.

If a fixed wing option is chosen then supersonic requirements demand a thin wing of low aspect ratio and in order to maintain good (L/D) at all M an advanced standard of wing design is necessary, more so than in the variable sweep case.

Whether the variable sweep or fixed wing, both will need some form of high lift enhancement to cover the full spectrum of design requirements.

3.1.2 Use of variable camber

Here the camber variation is confined to the leading and trailing edge regions only. The concept is illustrated using data on two dimensional aerofoils.

As mentioned in paragraph 2, one of the problem areas is achieving the high speed dash point, due to problems on the lower surface. This can be avoided to some extent by thickening the wing sections over the outer wing, thus increasing the radius of curvature near the leading edge and reducing lower surface suctions there, but at the expense of supersonic drag. However, if a variable camber system is adopted for a thin aerofoil, it is possible to deflect these upwards, relative to the high C_L design case, and, to obtain the same lower surface shape as on the equivalent thicker case. This is illustrated in Figure 5 and it should be noted that one obtains a smooth lower surface for the low C_L case and a smooth upper surface for the high C_L case. In each case the opposite surface will have concave regions but always associated with subcritical flow.

It is interesting to note that for a variable sweep aircraft this problem can be overcome simply by increasing wing sweep. Figure 6 shows the pressures at an outer wing station for 35° and 45° at a high speed dash condition. The strong shock on the lower surface for the 35° case has given way to a local leading edge suction at $\Lambda = 45°$ due to the effective reduction in free stream Mach number component normal to the wing leading edge. This infers that varicamber systems may have to be more highly optimised on wings of fixed sweep.

For the fixed wing option to be considered here, initial concept proving and design began with two dimensional aerofoils. Fig. 7 shows design pressure distributions for an advanced aerofoil.

The datum, high Mach number, high 'g' case corresponds to the 0°/0° leading and trailing edge setting which achieves an upper surface pressure distribution generating high lift for a small shock strength with a large amount of rear loading. As already mentioned, such a shape will have problems at low C_L conditions if this were to be achieved through a reduction in incidence only. However, by deflecting the varicamber system upwards one obtains a near subcritical distribution on both surfaces. The gain in drag rise Mach number is shown in Figure 8, where an intermediate case with up deflection of trailing edge only is shown. The boundaries imply that a smooth 'envelope' can be obtained with proper scheduling.

Such sections were developed using transonic computational methods with an allowance for viscous effects. A comparison of theory-exact potential flow equations coupled with an integral lag entrainment, boundary layer method - and experiment is shown in Figure 9. The comparison is good in terms of shock strength and position. However, final validation is always carried out in the wind tunnel.

4. Three Dimensional Design

4.1 Clean wing design

4.1.1 Various approaches

The simplest approach, if one has a 2D aerofoil in mind, is to factor this geometrically in some way and, provided that the wing planform taper is not much less than 0.5, this can be successful. Such an approach is shown in Figure 10, which compares predicted pressures at mid semi-span on a variable sweep wing (at $\Lambda = 35°$) with the 'equivalent' distribution obtained from the 2D pressures ('equivalent' here means keeping the same Mach number component normal to the isobars). The agreement on the upper surface is reasonable but there is a discrepancy on the lower. At wing root and tip such a procedure becomes less reliable, but it was adopted for the variable sweep wing considered here and for which results are given later. As implied earlier the effect of sweep changes may be more powerful than any highly optimised shaping at a particular wing sweep. Thus though the variable sweep design considered in this note was based on a good 2D section the 3D design treatment was of a simple nature, and can easily be improved. However, to consider the quantitative transonic flow development there is no alternative to a full transonic design.

Such an approach was adopted for the main fixed wing option ($AR = 3.3$, $\Lambda = 42°$, $\lambda = 0.3$) described below. Even here the design began by using the desirable features of the 2D aerofoil, particularly the upper surface pressure distribution. One could then proceed using either inverse methods, which produce the geometry from prescribed pressures or iteratively in a trial and error fashion, using direct transonic methods. The former approach was used and the resulting pressure distributions at a few spanwise stations are shown in Figure 11.

Here the main feature is the weak upper surface shock wave, with varicamber devices forming an implicit part of the design procedure. This primary design point was taken as the high M, high 'g' case corresponding to the $0^{\circ}/0^{\circ}$ flap settings and the inset sketch (not to scale) of the leading and trailing edge shapes clearly shows the concave regions on the lower surface, which give the pressure maxima in the lower surface distributions. The pressure distribution at a closely related 'g' value but at a lower Mach number is shown in Figure 12. Here, leading and trailing edge flaps are deflected to $+5^{\circ}$ and $+2^{\circ}$ respectively. The shock wave is much further forward, but still below the strength required to provoke boundary layer separation.

4.1.2 Aeroelastic Effects - off design cases

As implied, aeroelasticity can have a significant effect on wing design work. The primary effect is the change in streamwise wing twist due to wing deformation, with camber and anhedral effects playing a secondary role. Results of a parametric exercise, using a wing of conventional aluminium alloy structure, are shown in Figure 13. The aerodynamic required twist distributions at a high 'g' design condition were derived for a variety of planforms, which were representative of a fixed wing and variable sweep wing (at intermediate sweep) with perturbation of taper ratio. It was found that matching of required and aeroelastic twist could be obtained in both cases for taper ratio of around 0.35. Thus to some extent the planforms considered achieved natural tailoring of tip twist magnitude, but not necessarily distribution of twist along the span. An interesting point to emerge was that if tailoring, by use of suitable orientations of carbon fibre plies were considered, then there is more scope for this on the wing with the higher aspect ratio - Figure 14.

The actual fixed wing considered here - $AR = 3.3$, $\Lambda_{LE} = 42^{\circ}$, thus has a large degree of favourable aeroelastic effects, and would require only a mild degree of tailoring. The actual twist distribution is shown in Figure 15 for the high M, high 'g' design point - labelled high 'g' flight. Allowance for aeroelastic effects (early estimates) gave the original low 'g' shape whilst a more recent structural analysis gave the 'revised' jig shape, and'revised' low 'g' shape. Results, to be shown later, are for the original low 'g' shape. However, as implied from above, it should be possible to derive such a shape with only mild tailoring and possibly provide adequate stiffness for control effectiveness, flutter, etc.

Some of the benefits of tailoring, mainly the relief in lower surface suctions over the outer wing, are shown in Figure 16. Pressure distributions are shown for the high speed dash conditions, with varicambers deflected, appropriately, upwards. The left column of figures still has a high 'g' twist distribution but the right hand column has the corrected, or low 'g' twist distribution. The main feature is the reduced suctions near the wing tip for the low 'g' case, which leads to an increase in drag rise Mach number. For both distributions the effect of the up deflection of the trailing edge device is to reduce the rear loading over the outer wing and to reverse it over the inner wing.

4.1.3 Productionisation

Of the two basic options considered, the variable sweep and fixed wing, the former consisted of a constant wing section along the span, achieved by a simple geometric transformation, thus it was already effectively 'productionised'. The derived shape of the fixed wing however, consisted of a large number of control stations along the span which could lead to complications in manufacture, if it were ever considered for an aircraft, with possible twisted bowed spars, double curvature regions, non straight hinge line segments for control devices etc. Thus an exercise was put in hand to assess the effects of wing lines simplification on aerodynamic performance. This was done in two phases. The first phase was aimed at producing an equivalent wing shape which had only three control stations. The second phase went further and aimed to produce a wing with only two control stations. For consistency, the theoretical method used was again the small perturbation transonic wing-body method used in inviscid mode.

Figure 17 shows the approach adopted and consisted of making an allowance for aeroelastic effects, subtracting this from the ideal design shape, to obtain a 'jig' shape. This was then simplified, the aeroelastic effects reintroduced and the pressures re-calculated. This process was repeated using several simplified representations until satisfactory results were obtained.

The geometry of the basic shape is shown, along generator lines, by symbols in the top figure of Figure 18. They are characterised by a rapid change in spanwise slope over the rear of the wing due to the need to thin the inner wing in this region and hence reduce shock strength. The thinner feature of the inner wing could be represented by only three control stations as the bottom figure shows. However, this was not possible with a two control representation, since extrapolation of the inner wing generators to the tip produced excessive camber and very strong shock waves on the outer wing. Finally, an averaging technique was employed as shown in the bottom figure.

The resulting, predicted, pressure distributions are shown in Figure 19 for the high M, high 'g' design case. The three control station wing gives close agreement with the ideal case though shock waves are slightly stronger. For the two control case agreement is still reasonable, in that the same character is maintained, but the shock waves are further back on the chord. Thus the theoretical predictions implied that 'productionisation' could be achieved without, apparently, adverse aerodynamic effects.

4.2 Additions to the clean wing to improve high lift performance

4.2.1 Strakes

One way of improving high lift penetration is through the use of strakes. Since

methods were not available to design a strake in the presence of a wing two approximate approaches were adopted.

(a) Strakes were designed by calculating streamlines ahead of the wing at the high M, high 'g' condition and matching strake camber to the streamlines, thus hoping to produce 'non-interfering' type strakes at this selected condition at moderate C_L and shock dominated flow solution. It was hoped by this means to reduce the drag penalty usually associated with strakes. Two strakes were tried, one appropriate to the actual design incidence (Strake 1) and the other at half this incidence (Strake 2). They differ in their spanwise camber distribution as sketched in Figure 20.

(b) A larger, non cambered strake was used in further tests and was representative of a 'strongly interfering' type of strake known to give improved high C_L characteristics.

4.2.2 High Lift devices

Although only mentioned briefly tests were carried out for both variable camber type systems, representing flexible skin extents of approximately 8% chord, and slotted systems for both variable and fixed sweep wings. The shapes were derived using transonic methods for the non slotted devices and 'panel' type methods for the slotted cases.

5. Results

Since the design work relied heavily on the use of theoretical methods it is instructive to compare theory and experiment. This has been done in Figure 21 which compares a wing alone calculation (inviscid) with the wing + body test results, for the high M, high 'g' design case. Pressures are shown for the outer wing, and though the pressures over the rear part of the chord are reasonably well predicted there is a discrepancy over the front end. It is clear that in the experimental case the two shock system has merged into one at $\eta G = 0.678$, whilst the wing alone theory predicts two separate shocks. Including viscous effects in the theoretical calculation did not improve the comparison, simply having the effect of moving the shock wave forward (by up to 10% chord). However, including the body in the calculations brought about a marked improvement, as illustrated by the isobar plot of Figure 22. Now the front and rear shock waves merge at the same spanwise location for both theory and experiment. This is important since the merging region was part of the design philosophy of keeping it as far outboard as possible, in order to minimise the extent of the outer wing shock.

The results of the productionisation exercise are shown in Figure 23 for two Mach numbers. At both $M \doteq 0.5$ and $M = 0.88$ productionisation leads to a loss of approximately 3% in $(L/D)_{max}$, but with the discrepancy increasing at moderate C_L values, at the high Mach number. The results of the productionisation exercise is clouded by the fact that the simplified wing was tested on a model which had a different and wider fuselage, thus reducing exposed wing area and probably modifying drag due to lift values. If this was allowed for the reduction in (L/D) would not be as great. In any event the results are encouraging.

The effects of the strakes are shown in Figure 24 and Figure 25, the first of which compares isobar plots, strake off and strake on - at an incidence a few degrees above the design value. The isobar plots are similar in both cases thus confirming the 'non-interfering' aspects of the strake design. The agreement was even closer at the design incidence. The force data shown in Figure 25(a) also confirm the non-interference aspect in that both strakes contribute only a small drag penalty at moderate lift coefficients. Unfortunately, because of this, they are not so successful in alleviating the sharp break in the lift curve, evident in the strake off high Mach number case ($M = 0.88$).

The strongly interfering strake results shown in Figure 25(b) indicate that the break in the lift curve is improved here, but at the expense of a drag penalty at moderate C_L, though it was observed that this penalty decreased as Mach number increased. The data suggests that the lower the incidence for which a strake is designed as non-interfering then the greater will be its drag penalty but maximum lift ability will be improved. Thus the solution is, as usual, a compromise unless an articulated strake were to be considered.

Improvements from high lift devices are shown at two Mach numbers, for the fixed wing case, in Figures 26 and 27. Here the devices were representative of varicamber schemes with 8% flexible skin regions. Both a high 'g', and an aeroelastically distorted 1 'g' wing were tested. In Figure 26(a), (b) the C_L v α and (L/D) v C_L curves show the beneficial effect of leading and trailing edge droop. Values of (L/D) close to the optimum $(C_{Do} + C_L^2/\pi A)$, where CDo is taken from the 1 'g' case) are achieved for a wide range of C_L. At this Mach number the results imply that large deflections will further improve (L/D) values at high C_L. It is interesting to note that the low 'g' case, with flaps in the up position, gives more lift that the 8 'g' manoeuvre $0^\circ/0^\circ$ wing. This is because the reduced twist of the 1 'g' case outweighs the greater camber of the manoeuvre wing. The results are similar in nature for the high Mach number case in Figure 27(a), (b), but here the collapse of the $10^\circ/4^\circ$ and $5^\circ/2^\circ$ cases suggest that there is little to come from greater flap deflections at this Mach number. Here there is a larger fall off in performance below the 'optimum'.

Comparative data on various types of high lift device were obtained on the model with the variable sweep wing and are shown in Figure 28 for the 45° sweep case. The curves show (L/D) polar envelopes obtained from a range of deflections at two Mach numbers. At $M = 0.5$ - Figure 28(a) - use of varicamber improves (L/D) considerably but use of slotted devices increases this even more.

At M = 0.9 Figure 28(b) the same trend is evident but now the difference between datum, varicamber and slotted devices is much smaller. However, the slotted devices still offer an improvement in (L/D) at high C_L.

Finally comparison between the variable sweep and fixed wing option are shown, based on the same wing area, in Figure 29, again in terms of (L/D) capability. The $(L/D)_{max}$ comparison in Figure 29 (a) shows the beneficial effect of sweep (i.e. indirectly, span or aspect ratio) for the variable sweep wing and in Figure 29(b), which compares the ability to obtain a given 'g' for various Mach numbers, the same trend is apparent. In both figures the fixed and variable sweep case merge at the higher speeds, since the variable sweep in this case suffers more wave drag, which cancels out the benefit of its greater aspect ratio. However, over the major part of the Mach number range the variable sweep option is superior. As usual, the final choice must be on the basis of judging aerodynamic advantages against potential weight and cost penalties.

6. Final Remarks

It has been shown that the achievement of a given set of often conflicting requirements can be sought in many different ways. Use of powerful mixed flow methods operating in wing + body mode can lead to configurations with good (L/D) characteristics over a wide (M, C_L) range. Use of variable sweep wings is attractive from the purely aerodynamic point of view and give improved performances over a fixed wing at low to moderate subsonic Mach number. At high subsonic speeds the situation is not so clear with a trade off between the increased aspect ratio of the variable sweep swing and reduced (t/c) of the thin wing, but the variable sweep option probably leads to a smaller wing with lower drag and better gust response at low altitude high speed conditions.

High lift devices, in particular varicamber scheduled with (M, α), can be used to match the various requirements if built into the wing from the outset. In particular the trailing edge is a powerful device for improving high lift without compromising high speed low level flight, whilst the leading edge can be used to improve both high and low lift without supersonic penalty. Slotted devices offer a further improvement at high C_L.

Aeroelastic effects generally have a favourable influence on wing performance, from the wing designers point of view. To some extent this occurs naturally but some 'tuning' can be done by aeroelastically tailoring the wing to match the particular aerodynamic twist requirements, particularly with carbon fibre composites.

It has been shown that it is possible, to design non-interfering strakes which have only a very small drag penalty at low to moderate C_L. However, this type of strake is not so successful in penetrating the high incidence regime. Strongly interfering strakes are better for this purpose, but usually at the expense of a drag penalty. The ideal situation, aerodynamically, would be to have a varicamber/articulated strake.

When practical constraints were considered it was possible, in this particular instance, to simplify the ideal wing shape without incurring much aerodynamic penalty. Theoretical calculations imply that a further simplification could be possible, though it is not claimed that this would be a general result.

Acknowledgments

The work described is taken from a broad based exercise undertaken by BAe (Warton and Brough Divisions) and mainly funded by the M.O.D. through a series of research contracts.

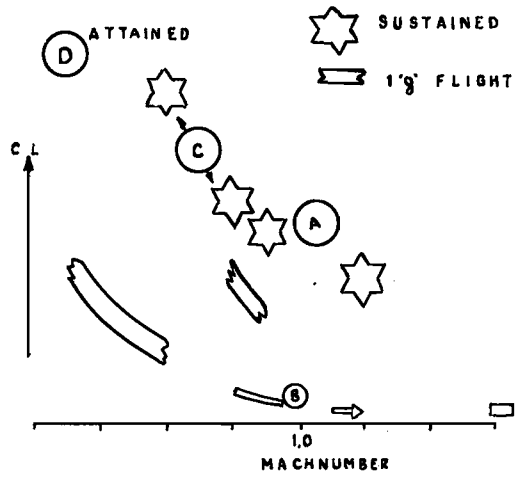

FIG.1. TYPICAL DESIGN REQUIREMENTS.

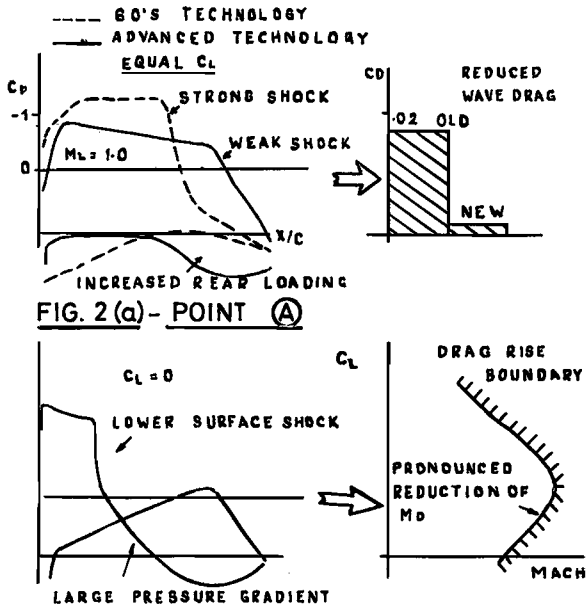

FIG. 2 (a) - POINT (A)

FIG 2 (b) - POINT (B)

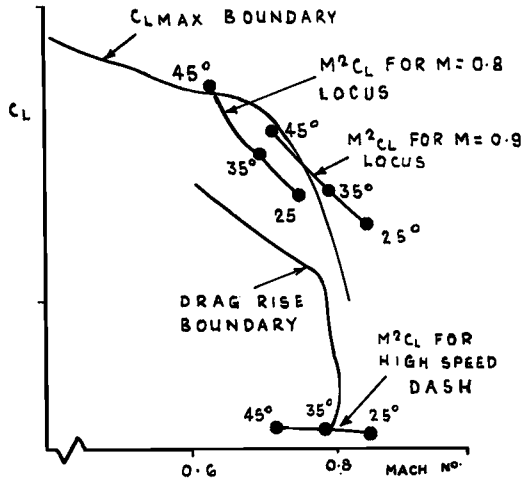

FIG.3 INFLUENCE OF WING SWEEP ON DESIGN POINTS.

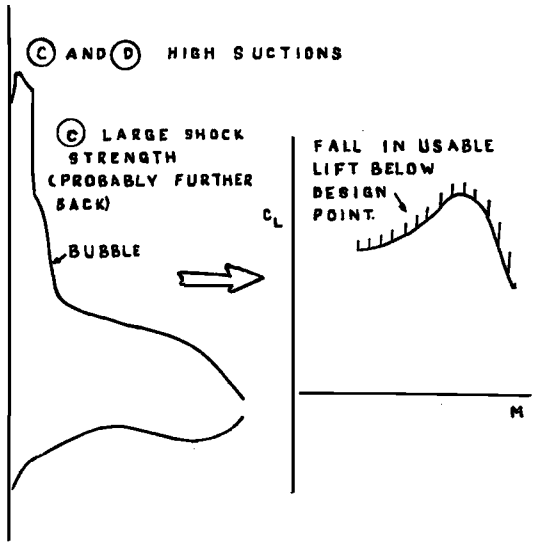

FIG. 2 (c) - POINTS (C) AND (D)

FIG. 2 - MAIN FLOW FEATURES

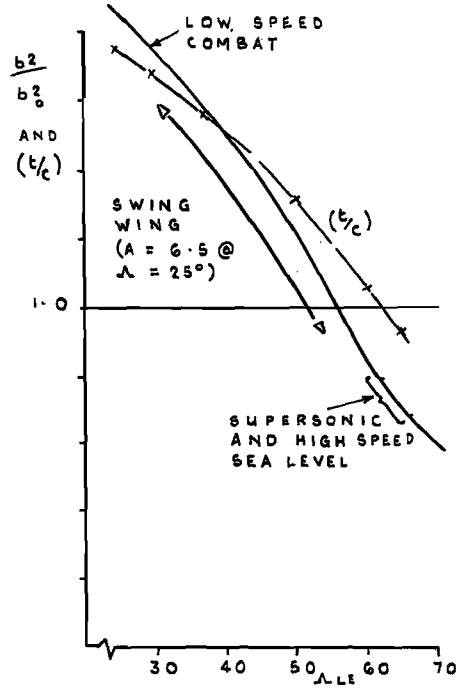

FIG.4 SPAN SQUARED AND THICKNESS FOR SWING WING COMPARED WITH FIXED WING (EQUAL AREAS)

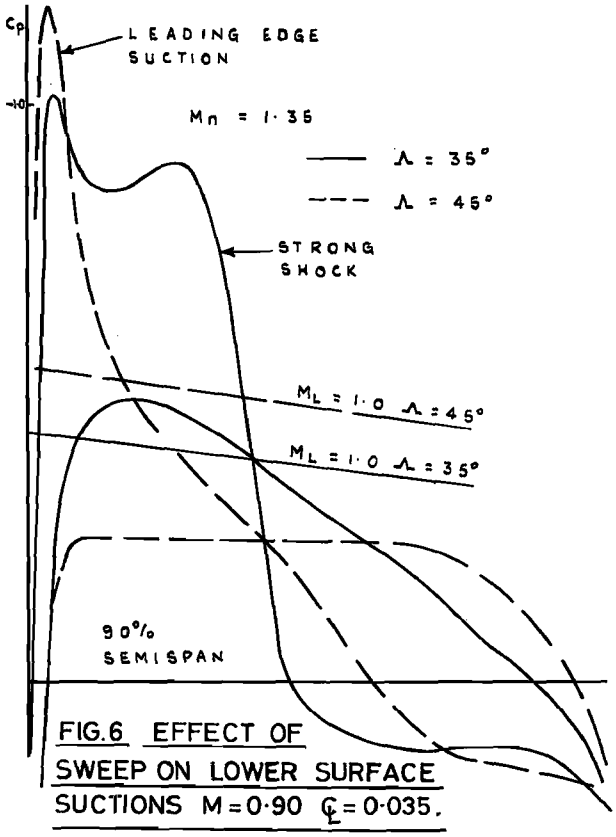

FIG.6 EFFECT OF SWEEP ON LOWER SURFACE SUCTIONS M=0·90 C_L=0·035.

SHAPE OBTAINED BY MATCHING HIGH LIFT UPPER SURFACE WITH LOW LIFT LOWER SURFACE

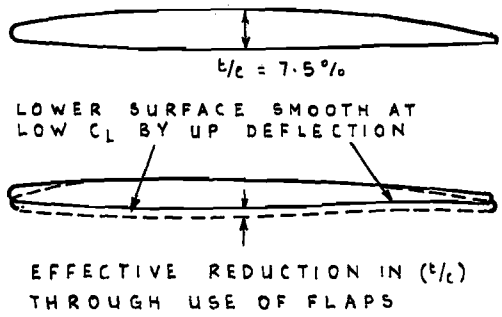

FIG. 5 VARIABLE CAMBER–EFFECTIVE (t/c) REDUCTION.

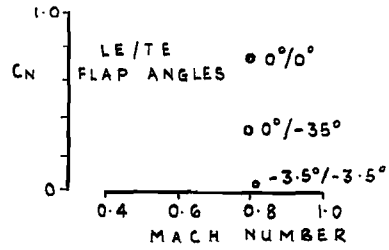

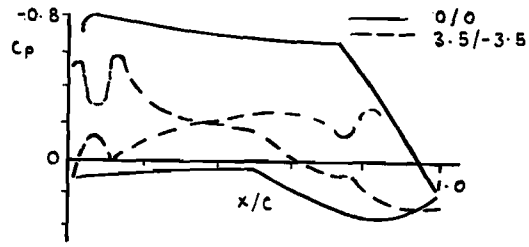

FIG. 7. THEORETICAL PRESSURES

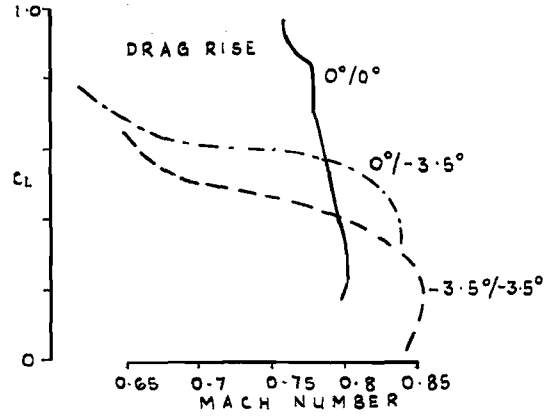

FIG 8 EXPERIMENTAL BOUNDARIES

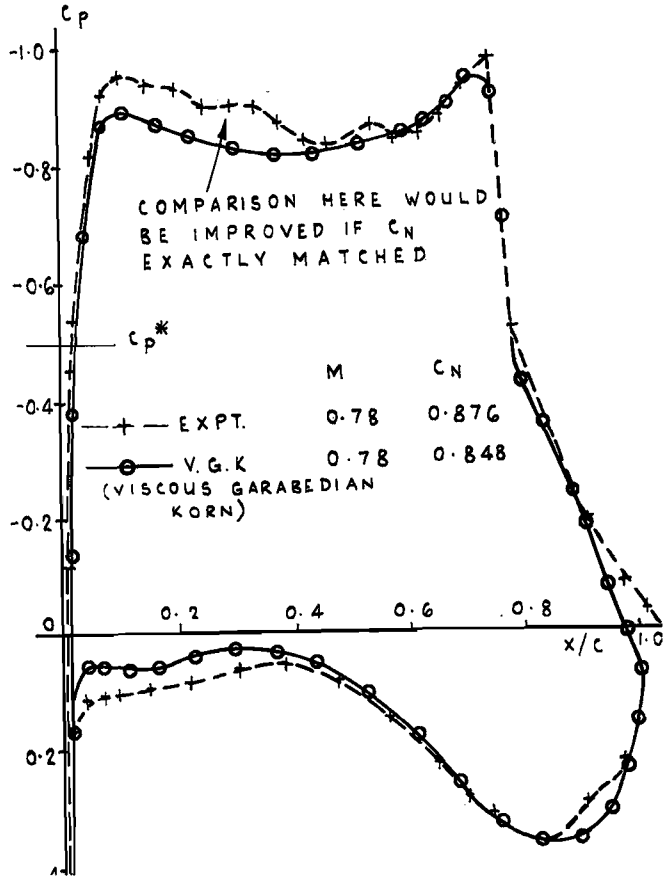

FIG. 9 2D THEORY V EXPERIMENT

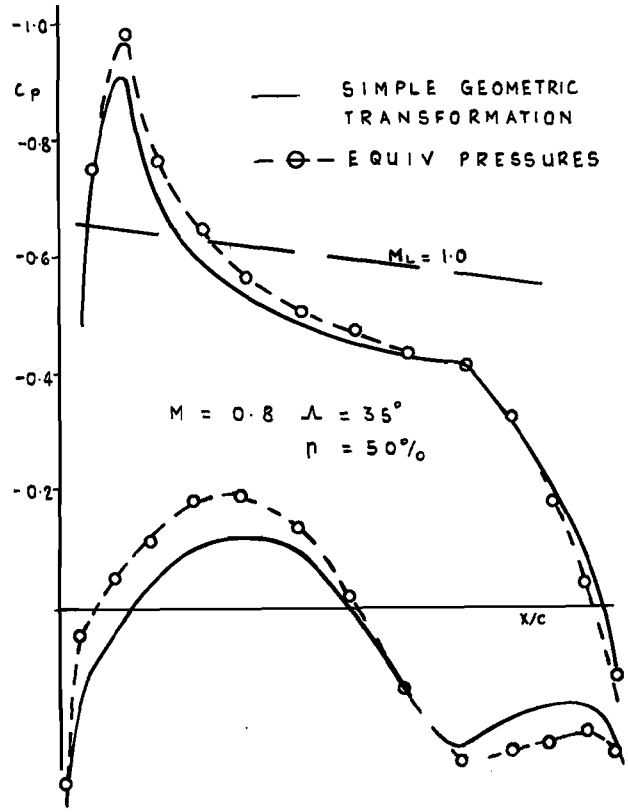

FIG.10 2D TO 3D VIA SIMPLE GEOMETRIC TRANSFORMATION

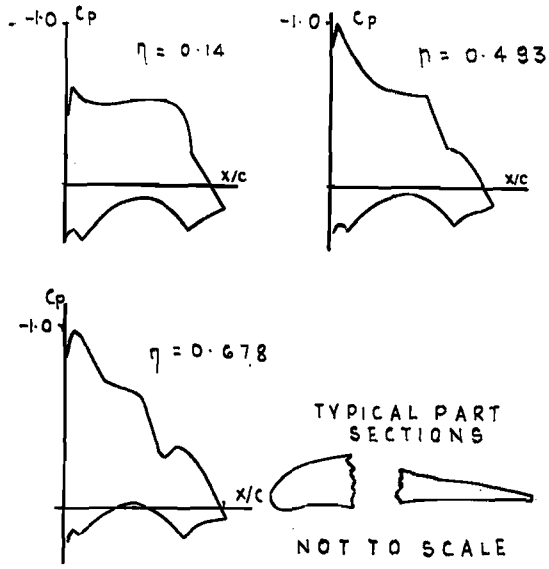

FIG 11 PRESSURE DISTRIBUTION AT MAIN DESIGN POINT

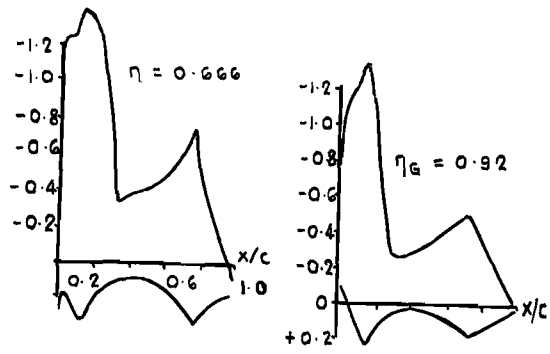

FIG .12 PRESSURE DISTRIBUTION AT LOWER M HIGH C_L

$\Lambda_{LE} = 5°$

$\Lambda_{TE} = 2°$

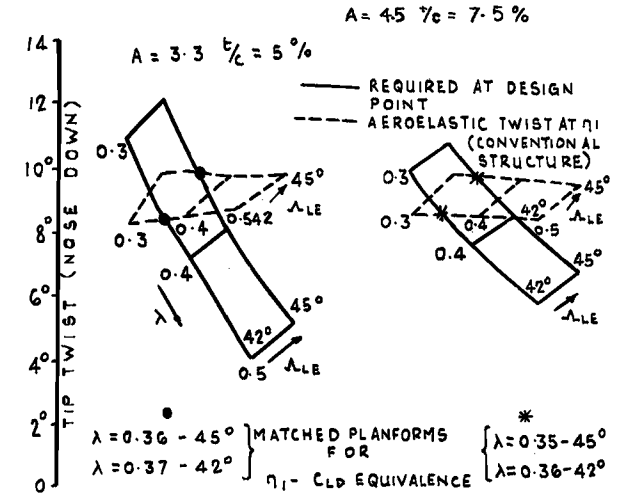

FIG .13 COMPARISON OF REQUIRED TWIST AND AEROELASTIC DUE TO BENDING

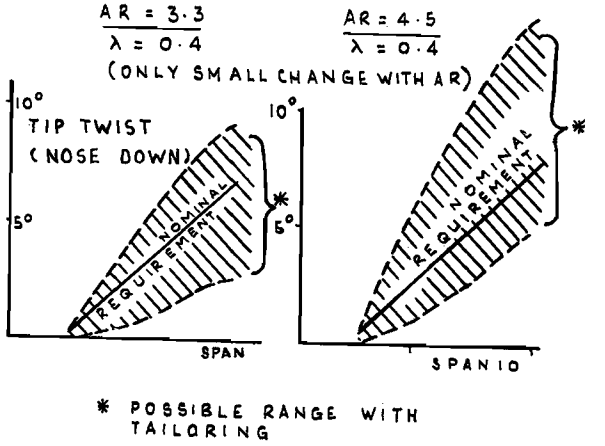

FIG .14 EFFECT OF ASPECT RATIO ON AEROELASTIC TAILORING BOUNDARIES

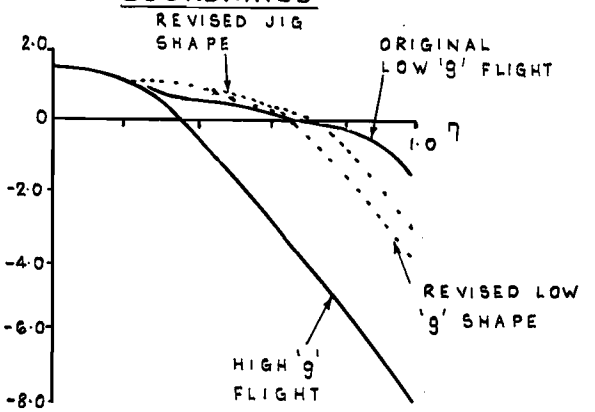

FIG 15 AEROELASTIC EFFECTS ON WING TWIST

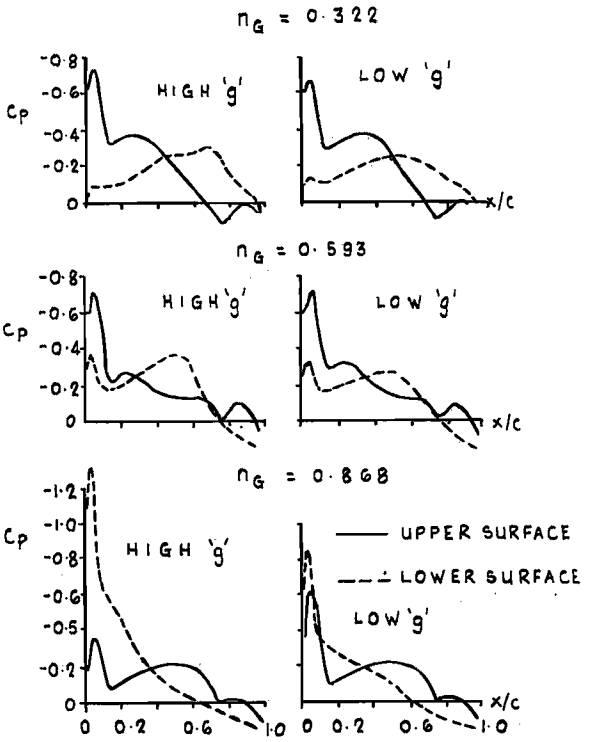

FIG. 16 PRESSURE DISTRIBUTION FOR FLAP DEFLECTIONS -5/-4 HIGH M-LOW CL-

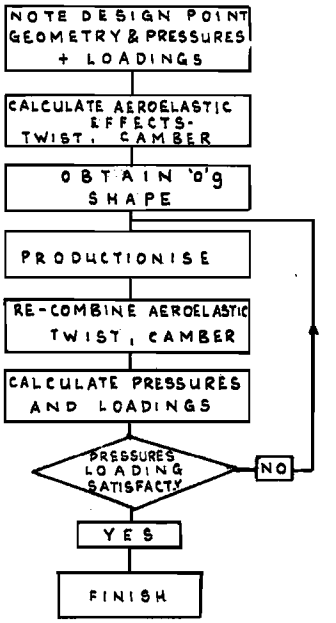

FIG. 17

PRODUCTIONISATION PROCEDURE

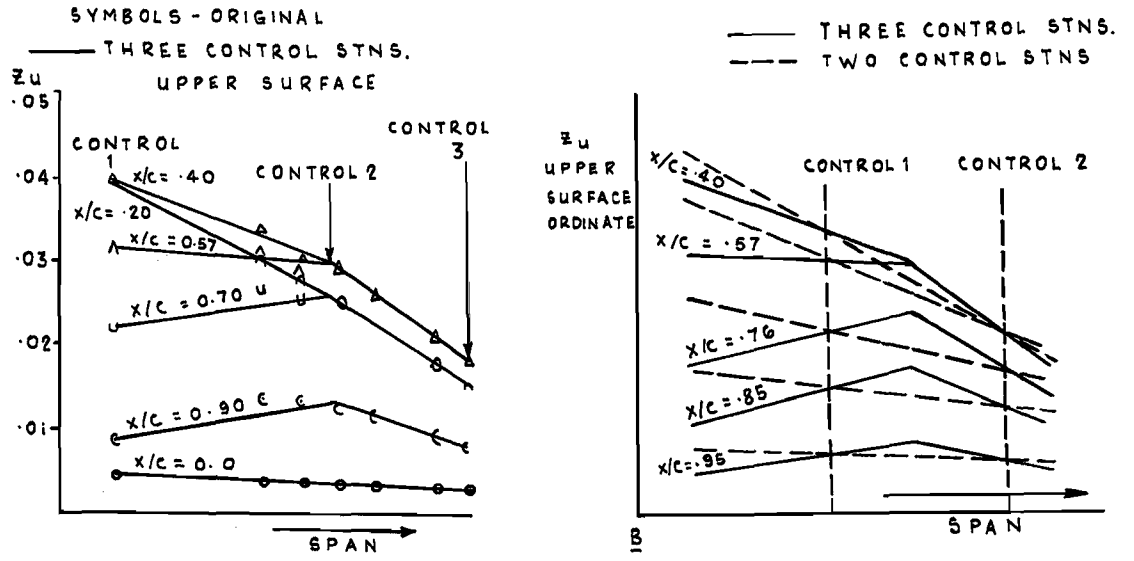

FIG 18 GEOMETRY

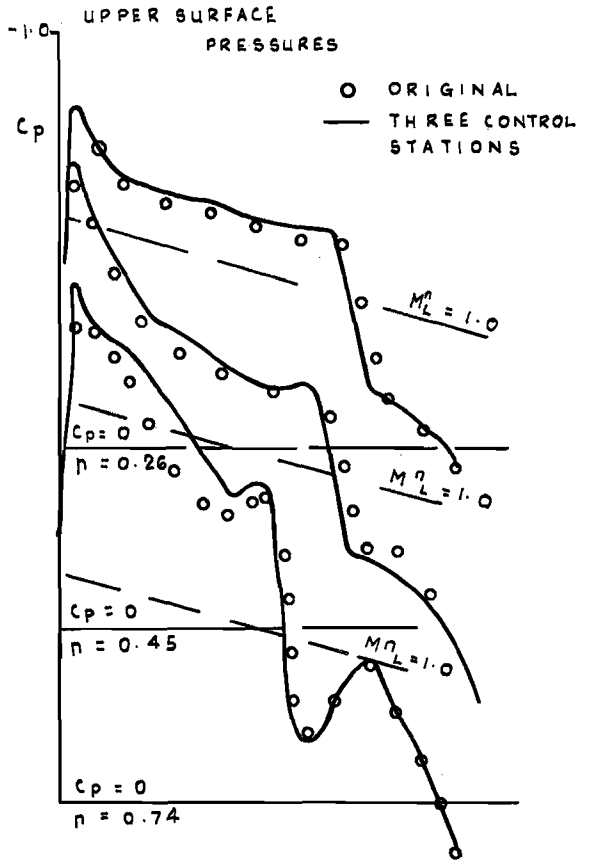

FIG 19 A ORIGINAL COMPARED WITH THREE CONTROL STATION WING

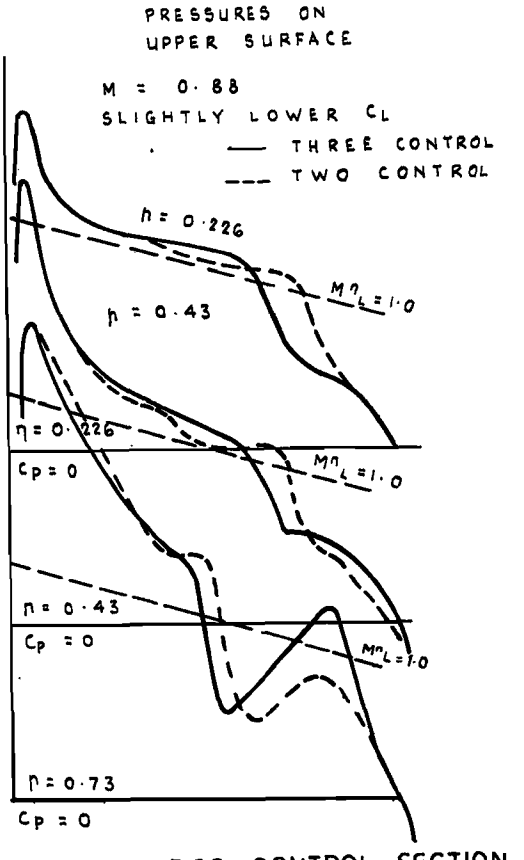

FIG 19 B THREE CONTROL SECTION WING COMPARED WITH TWO SECTION WING

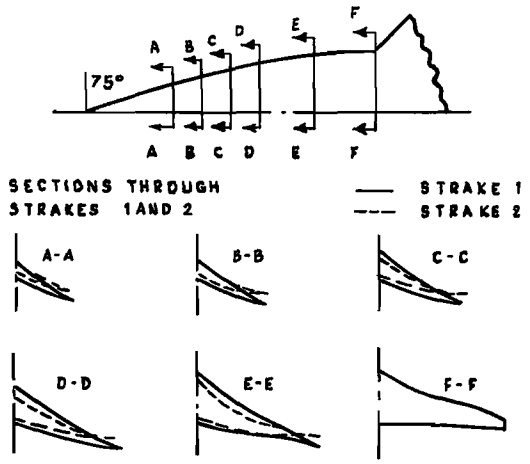

FIG. 20. NON INTERFERING STRAKE GEOMETRIES

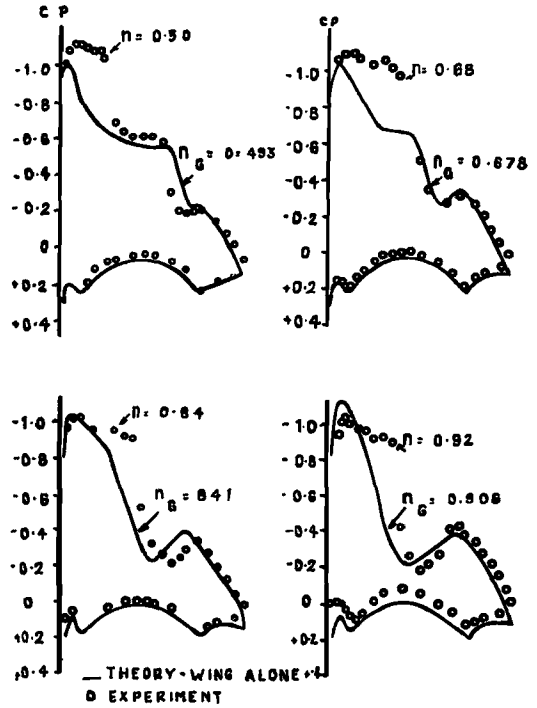

FIG. 21. PRESSURE DISTRIBUTIONS AT M=0·88

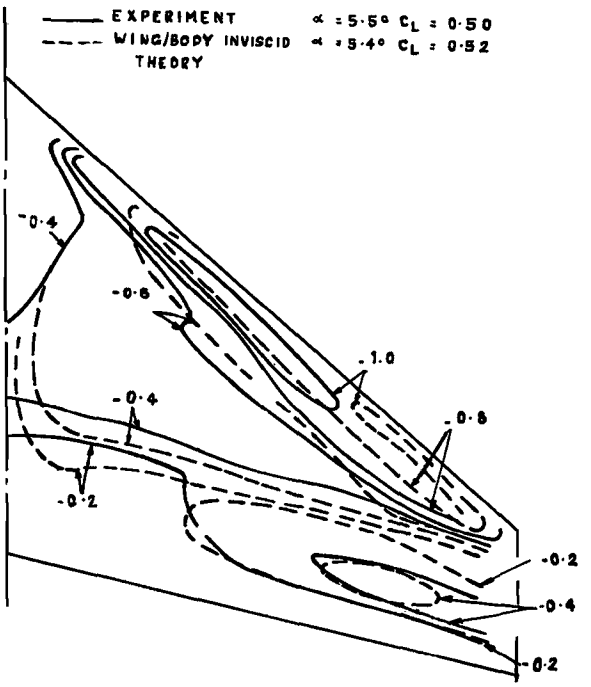

FIG. 22. ISOBARS AT M = 0·88

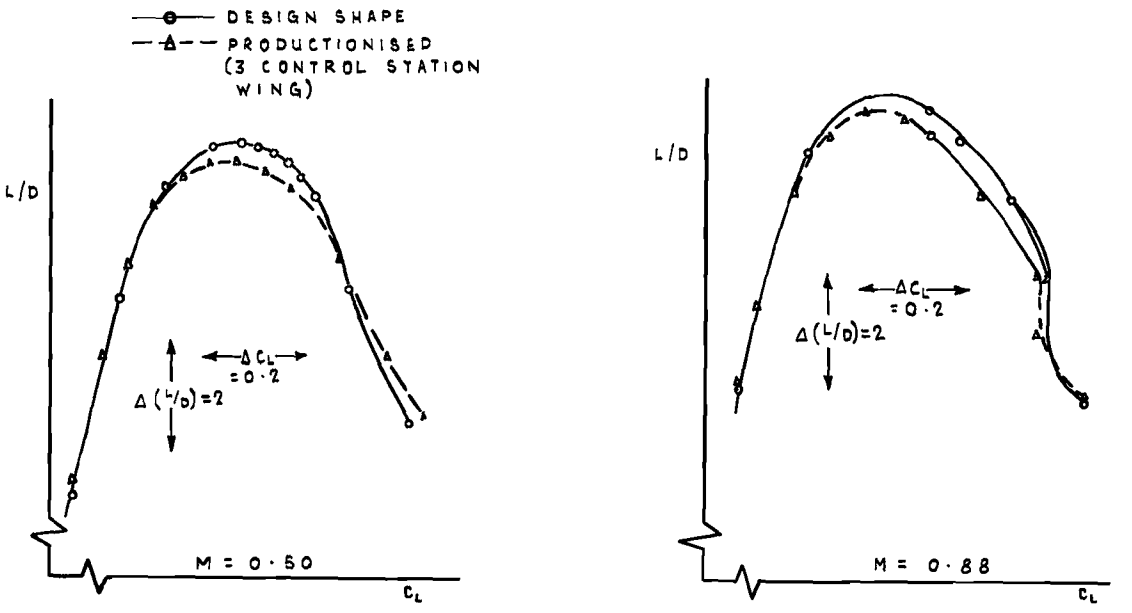

FIG. 23 EXPERIMENTAL RESULTS

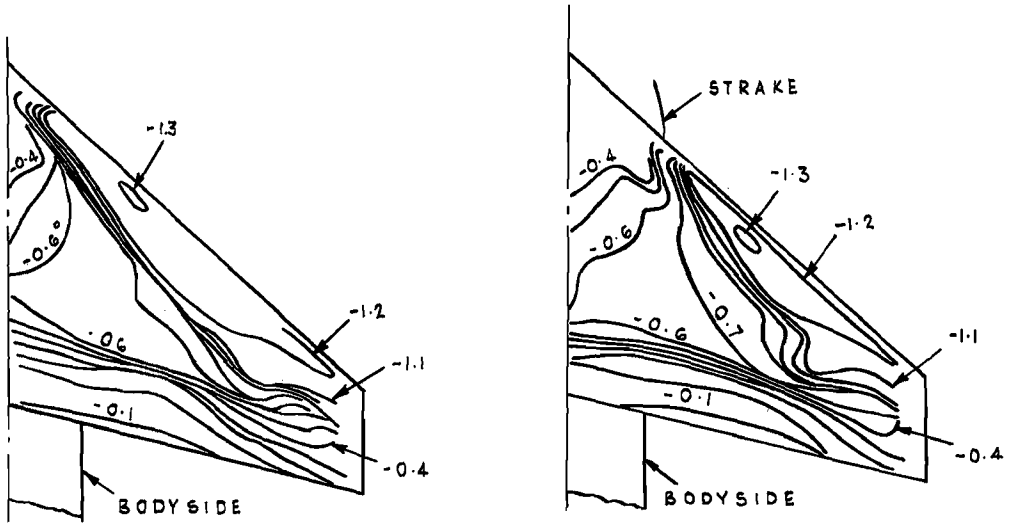

STRAKE OFF STRAKE ON

FIG. 24 ISOBARS. STRAKE OFF AND ON M = 0.88 α = 8.8°

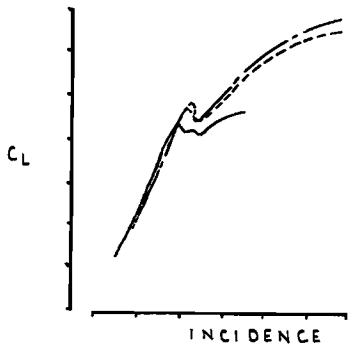

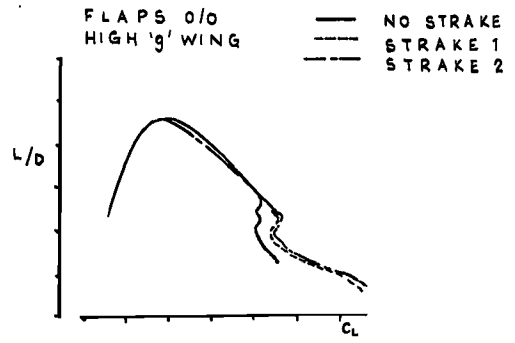

FIG.25 (a) EFFECT OF STRAKES AT M = 0·88
-NON INTERFERING-

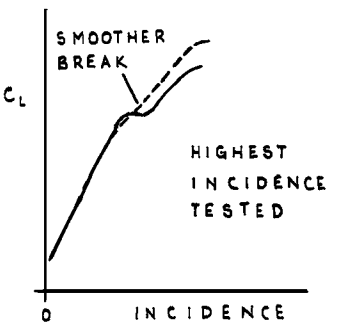

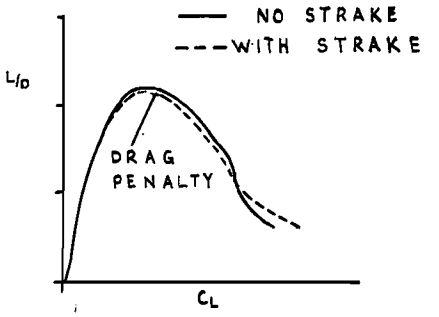

FIG 25 (b) EFFECT OF STRAKES -INTERFERING-

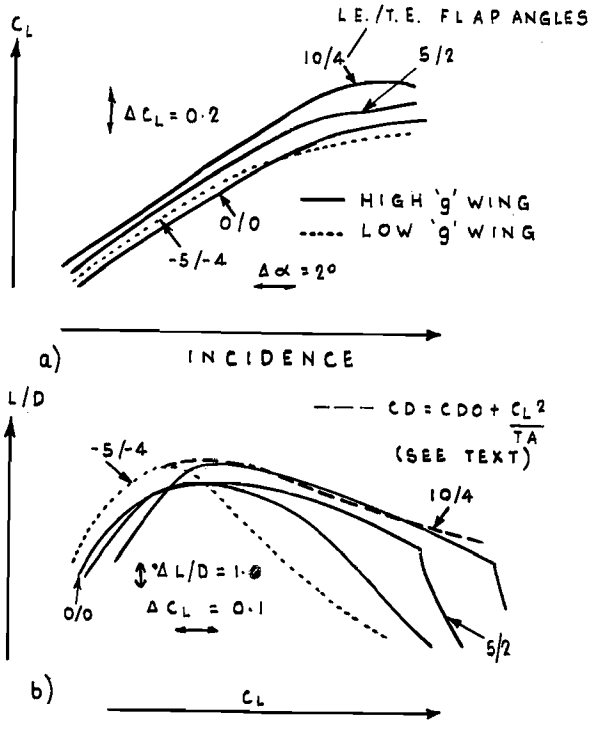

FIG 26 LIFT AND DRAG AT M=0·65

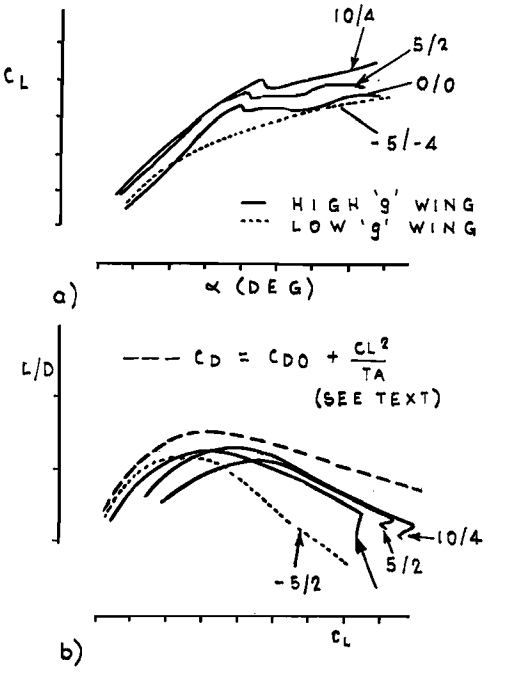

FIG 27 LIFT AND DRAG AT M = 0·88

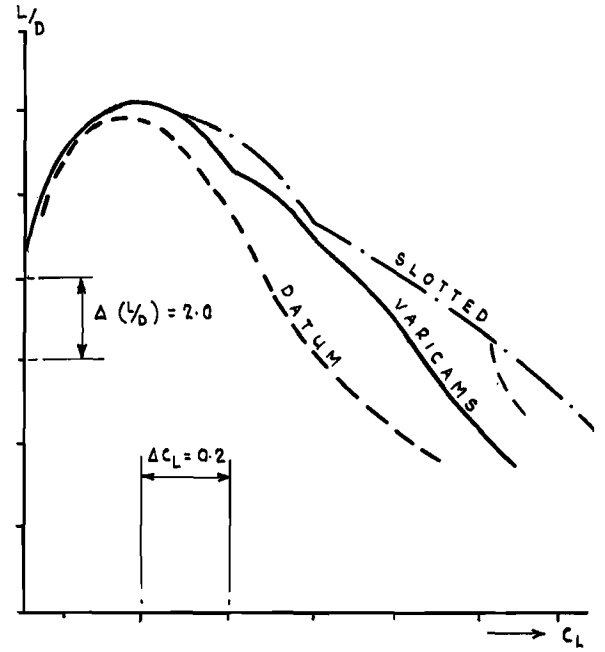

FIG. 28 (a) VARICAMBER V SLOTTED

Λ_{LE} = 45° M = 0·50

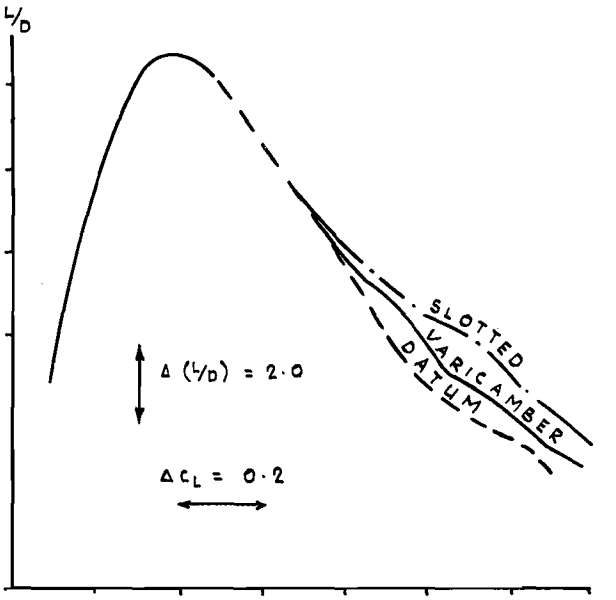

FIG 28 (b) VARICAMBER V SLOTTED

Λ = 45° M = 0·90

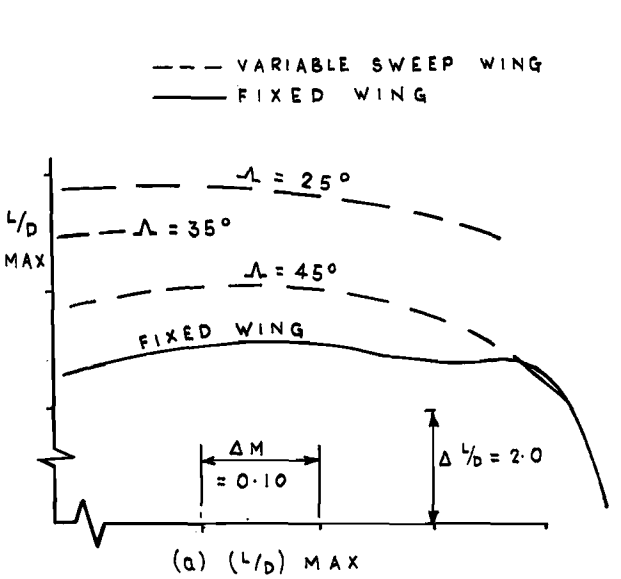

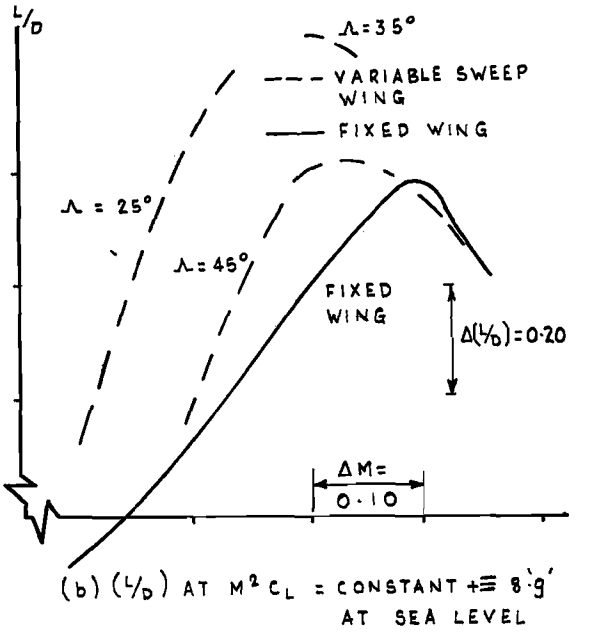

FIG 29 COMPARISON OF VARIABLE SWEEP AND FIXED WING RESULTS —